Hydrophobic Hydration and the Formation of a Clathrate Hydrate

Daniel T. Bowron,[1,*] Adriano Filipponi,[2] Mark A. Roberts,[1] and John L. Finney[1]

[1]*Department of Physics and Astronomy, University College London, Gower Street, London, WC1E 6BT, United Kingdom*
[2]*Dipartimento di Fisica, Università dell'Aquila, Unità di Ricerca INFM, Via Vetoio, 67010 L'Aquila, Italy*

We report a direct comparison of the local structure of the hydrophobic hydration of krypton in both the liquid and solid states by the extended x-ray absorption fine structure spectroscopy technique. The evolution of an ordered hydration shell of the nonpolar gas moiety is followed as the liquid to solid phase transition progresses. The formation of a clathrate cage structure from the more disordered liquid state hydration shell is clearly demonstrated. [S0031-9007(98)07579-6]

Gas hydrates are an interesting and very important class of materials that often display unusual properties [1]. The structural processes involved in the formation of these materials are currently a topic of great interest for many reasons; for example, there are significant quantities of valuable natural gas resources stored in this form [2].

The crystalline structures of the gas hydrates have been well characterized. Generally the structures are of the cagelike type-I or type-II clathrate structures, depending upon the size of the "guest" gas molecules [3,4], and which stabilize the lattice through nonbonding repulsive interactions [5,6]. These structures have a principle building block which is the pentagonal dodecahedron of radius 3.9 Å. As this is not a space filling polyhedron, the crystalline form of these hydrates contains a second (larger) polyhedra to form the lattice [4]. Though the type-I structure has a smaller large cage size than type II, the smallest guests, e.g., argon, krypton, and oxygen, tend to form the latter, probably because the ratio of small to large cages is higher [7].

Here we report an investigation of the hydrate formation process using extended x-ray absorption fine structure (EXAFS) spectroscopy. The EXAFS probe is intrinsically short ranged and element specific; in this case we investigate the local structure around krypton atoms on either side of the liquid to solid phase transition, where the structural signal is dominated by krypton to water oxygen correlations. EXAFS is an ideal microscopic probe for the comparison of the local structure around the Kr atom in the two phases due to its insensitivity to the onset of the long range order in the crystalline phase.

The structural nature of nonpolar gas hydration is particularly relevant to the still controversial topic of hydrophobic hydration and the associated hydrophobic effect, by which nonpolar solute moieties associate in the aqueous environment. The direct comparison of the local structure between the liquid state and solid state hydration of a nonpolar gas provided by this experimental study allows us to make a direct evaluation of the often-misinterpreted iceberg model of hydrophobic hydration suggested by Frank and Evans in 1945 [8]. They pos-

tulated that the water hydrating such solutes might be perturbed in the direction of greater crystallinity when compared with that found in the pure bulk solvent.

This model [8] has subsequently generated a great deal of interest among experimental and theoretical workers in the field, and has become the "standard model" of hydrophobic hydration [9]. However, it remains unverified experimentally, due in significant part to the lack of any direct comparison between the solid and liquid state hydration structures of nonpolar solutes in water.

The measurements presented in this letter were made on a Kr-water mixture at 110 bars pressure and at temperatures below 10 °C. The experiment was performed on the x-ray absorption spectroscopy beam line, BM29, at the European Synchrotron Radiation Facility (ESRF). The synchrotron was operating in 2/3 fill mode with typical beam currents of 180 mA and an electron energy of 6 GeV. The experimental station was equipped with Si(311) monochromator crystals detuned by 40% for harmonic rejection, and ion chamber detectors operating with Ar/He gas mixtures optimized for data collection at the Kr K absorption edge, 14.3236 keV. The sample was illuminated by an x-ray beam of dimension 200 μm vertical by 7.0 mm horizontal size. In this configuration an energy resolution of 0.6 eV was attained, for comparison with the intrinsic core hole width of 2.7 eV (FWHM).

The sample was contained in a pressure cell designed to operate in the 1 to 120 bars pressure range and −20 to 100 °C temperature range. The sample was delimited by two epoxy resin x-ray windows to a 1 mm gap; these windows were suitably transparent for EXAFS measurements above 12 keV. The cell was first filled with outgassed deionized water, to the level of the x-ray window. It was important that the gas/water interface be as close to the x-ray beam path as possible, so as to avoid the region of the sample that was to be probed from becoming isolated from the pressurizing gas by a surface layer of clathrate ice. The cell was sealed using a copper gasket and pressurized to 110 bars with Kr gas of 99.998% purity. This cell was then placed within a thermostatic chamber and cooled by means of a nitrogen gas flow through a heat exchanger

immersed in a mixture of liquid nitrogen and ethanol. A consecutive series of spectra (lasting about 20 min each) were collected while gradually cooling the sample below the solidification temperature. The first set of spectra were identical and representative of the solution phase. After a few transition spectra, the spectral signal stabilized to another shape that we have assigned to the solid clathrate structure. A selection of three representative spectra showing the liquid, solid, and transitional phases are shown in Fig. 1. The averages of the liquid and solid phase spectra corresponding to average temperatures of 4 ± 5 and $-5 \pm 5\,°C$ have been used in the subsequent analysis.

In Figs. 2 and 3 we report the XAS spectra for krypton gas in cold water and in the solid state gas hydrate, respectively. The x-ray absorption fine structure is defined as $\chi(k) = (\alpha - \alpha_{bkg})/\alpha_{nor}$ and the photoelectron wave vector modulus is $k = \sqrt{2m(E - E_e)}/\hbar$. α_{bkg} accounts for the nonstructural atomic background, the normalization function α_{nor} is taken as a smooth atomic cross section model for Kr scaled by the edge discontinuity, and E_e is the energy of the inflection point at the Kr K-edge. For both the liquid and solid state data, the double-electron excitation background was removed as in our earlier investigation [10]. The liquid to solid phase transition is associated with small but significant changes in the spectrum. In particular, in the solid state spectrum higher frequency contributions are apparent, arising from the longer range order. The gain in amplitude of the solid state signal over that of the liquid is limited due to the large thermal and configurational disorder present in the enclathrated krypton environment.
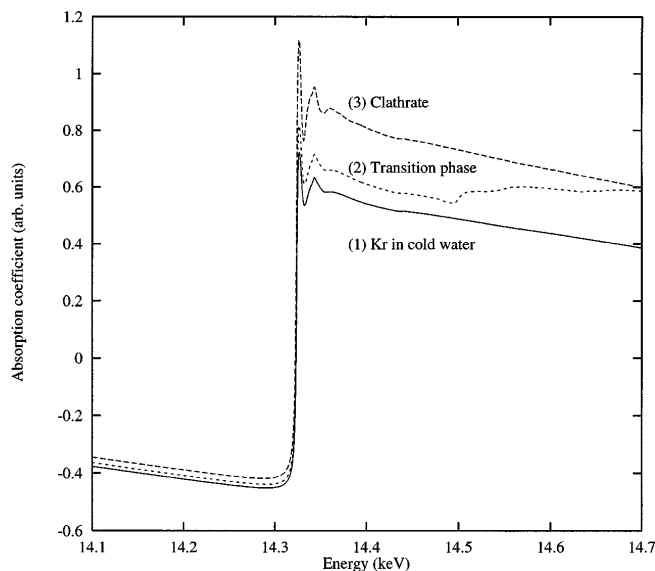
The procedure adopted for modeling the x-ray absorption spectra is based on a previously published analysis scheme [11], and, for the liquid state data, a radial distribution methodology specifically designed to deal with disordered systems [12,13]. In the solid state the two-body signal was modeled as the sum of four shell contributions due to Kr-O and Kr-Kr correlations in small and large cages. To account for the higher frequency signal component seen in the clathrate data set, two collinear Kr-O-O three-body correlations were found to be necessary. These are signals $\eta_1^{(3)}$ and $\eta_2^{(3)}$ in Fig. 3, calculated combining the Kr-O correlations of the first shells (associated with signals $\gamma_1^{(2)}$ and $\gamma_2^{(2)}$) with the collinear O-O arrangements radially oriented about the center of the small and large cages. This model agrees with the known type-II clathrate structure and therefore allows us to identify this high frequency component as a signature of the transition to the solid state.

The structural parameters and associated uncertainties refined for the crystalline hydrate system are summarized in Table I. The modeling of the structural parameters was pursued through the initial refinement of the small and large cage radii, signals $\gamma_1^{(2)}$ and $\gamma_2^{(2)}$ in Fig. 3. The radius of the small cage was fixed at 3.902 Å, and provided the principal anchor parameter for the structural refinement (a value that would be consistent with either the type-I or type-II hydrate structures). Following this constraint, the radius of the large cage component was found to refine to a value of 4.9 Å. This value is most consistent with a type-II hydrate structure. The uncertainties in the refined crystal structure are significantly less than those for the liquid state [10]; this is particularly true in the 4 to 5 Å range. The presence of the three-body Kr-O-O correlations proved crucial to the successful modeling of this structure as they account for the bulk of the high frequency component observed in the experimental signal.
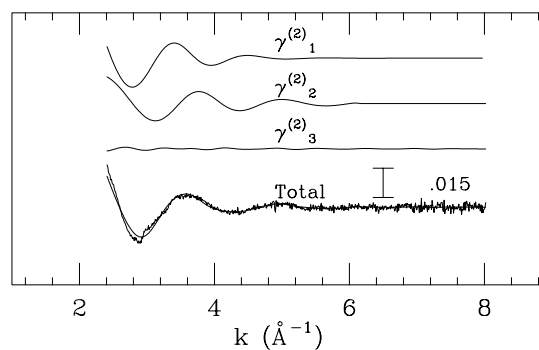

FIG. 1. X-ray absorption spectra at the Kr K-edge of a Kr-water system pressurized to 110 bars and at temperatures below 10 °C. The three spectra correspond to Kr in water in the liquid state (bottom), Kr in water in the solid clathrate ice (top), and an example of a spectrum taken during the liquid to solid transition.

FIG. 2. $k\chi(k)$ weighted x-ray absorption spectrum and model fit for krypton gas in cold water ~5 °C and at ~110 bars pressure. From top to bottom are shown the first and second shell contributions to the radial distribution function first peak, the signal contribution required to model the long range bulk density of the system, and, lastly, the experimental data and resulting model signal, respectively.
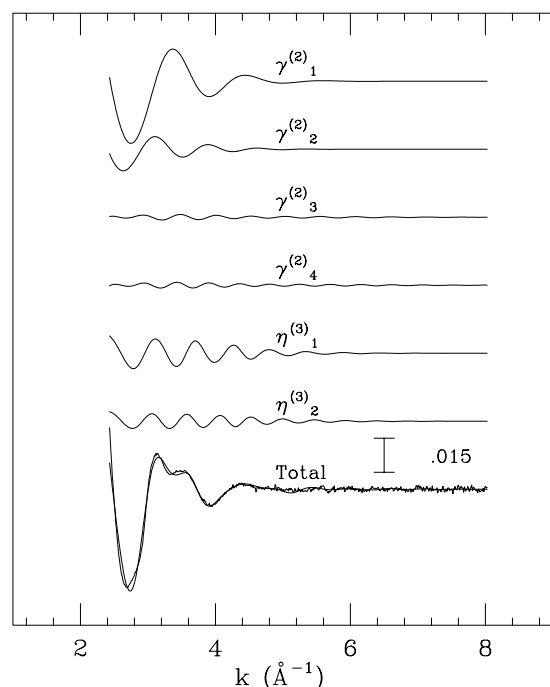
FIG. 3. $k\chi(k)$ weighted x-ray absorption spectrum and model fit for the krypton gas hydrate, at $\sim -5\,°C$ and at ~ 110 bars pressure. From top to bottom are shown the small cage Kr-O signal, the large cage Kr-O signal, the small cage-small cage Kr-Kr signal, the small cage-large cage Kr-Kr signal, the small cage Kr-O-O 180° three-body contribution, the large cage Kr-O-O 180° three-body contribution, and, lastly, the experimental data and total six signal model fit.

As a result of this analysis it is possible to compare the short range of the Kr-O partial radial distribution functions of the solution and clathrate structures, a comparison which cannot easily be made by any other technique. For consistency of comparison between the solid state and liquid state data, the empirical fitting parameters E_0 and S_0^2, which define the alignment between the experimental and theoretical energy scales and the overall amplitude reduction factor, were refined for the solid state system and transferred as constants to the refinement of the liquid state system. The results are shown in Fig. 4. The atomic
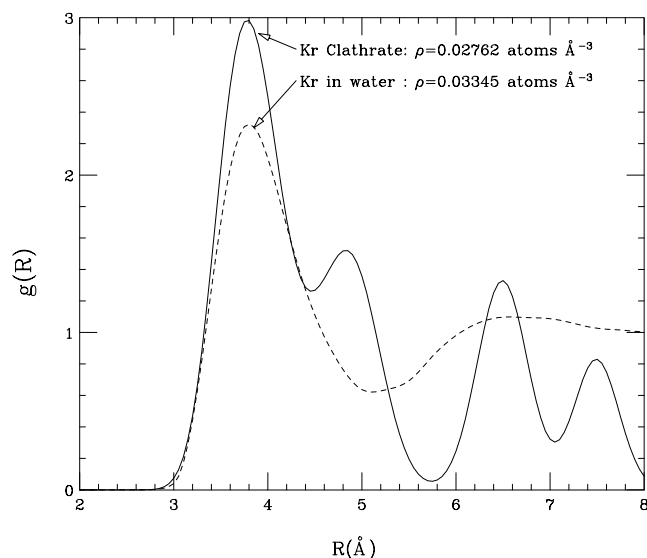

FIG. 4.   Refined Kr-O partial radial distribution function derived from the liquid state EXAFS spectrum at $\sim 5\,°C$ and ~ 110 bars and the comparable distribution function determined from the solid crystal data.

density of oxygen sites used for calculating the liquid state $g(r)$ was $0.033\,45$ atoms $Å^{-3}$ and that for the crystalline state was $0.027\,62$ atoms $Å^{-3}$. For the solid state the $g(r)$ includes the two first shell contributions from the small and large cages and the corresponding second O shells derived from the three-body Kr-O-O correlations. Further O atoms at distances higher than about 7 Å are not accounted for, and therefore the correct long range limit of $g(r) = 1.0$ is not approached. The comparison of the two $g(r)$s below 7 Å is, however, meaningful.

Figure 4 therefore allows us to compare the local structure for the solid and liquid state hydrophobic hydration of a noble gas atom. The first peak in the radial distribution function occurs at the same distance of 3.8 Å, indicating that the size of the liquid state hydration shell is directly comparable with the small cage of the type-II clathrate hydrate. On integration, the number of water molecules involved in the first coordination shells of the liquid and

TABLE I. Refined values of the main parameters used to fit the crystalline clathrate hydrate structure. The first shell distance was fixed at 3.902 Å while the first and second shell coordination numbers were constrained by using the relationship $N_{sc} = (1 - x) \times 20$ and $N_{lc} = (x) \times 28$, where 20 and 28 are the number of water molecules required for the small and large cages of the type-II clathrate structure (Scage and Lcage), respectively. Within this constraint, the parameter x is the fraction of large cages, ideally $\frac{1}{3}$, and which refined to a value of 0.35. These first two shells were modeled allowing for a degree of asymmetry, characterized by the parameter β for a Γ distribution. The other shells were modeled within a Gaussian approximation while their coordination numbers were constrained to the crystallographically accepted values.

Shell	Coordination number (atoms)	R (Å)	σ^2 ($Å^2$)	β
Small cage Kr-O	13.05	3.902 (fixed)	0.12 ± 0.06	0.3 ± 0.3
Large cage Kr-O	9.73	4.9 ± 0.1	0.10 ± 0.05	-0.1 ± 0.5
Scage-Scage Kr-Kr	4.0 (fixed)	6.4 ± 0.3	0.05 ± 0.02	$\cdots$
Scage-Lcage Kr-Kr	8.0 (fixed)	7.3 ± 0.1	0.05 ± 0.02	$\cdots$

solid hydrates are the same—in the 2.6 to 4.5 Å range ~13 water molecules are found in the liquid state and ~12.5 water molecules in the solid. However, the higher degree of ordering in the hydration shell of the solid results in the sharper features of the crystalline radial distribution function. In the crystalline system the full width at half maximum of the first peak is found to be 0.9 Å, whereas in the liquid state it is closer to 1.1 Å. This observation suggests that the average orientational configurations of water molecules in contact with the gas solute in the liquid state deviate from the largely tangential orientational configurations adopted in the clathrate cage structure; i.e., a hydration "cage" exists in the liquid, but it is more loosely defined than in the solid state system. It is interesting to note that the determined coordination numbers indicate that, on the transformation from the liquid to the solid state, one extra water molecule is drawn into the 4.5 to 5.1 Å distance range to form the large cage structure with ~18 water molecules found in the liquid state and ~19 in the clathrate, although the total number of water molecules in the 2.6 to 5.7 Å range remains constant at ~22.5.

Of note is the observation that the position of the large cage hydration shell coincides with the minimum in the liquid state radial distribution function. Molecules that contribute to the formation of the solid from the liquid state must therefore be drawn into this local vicinity of the gas atom as the cage structure is established in the solid. This raises the interesting question as to whether the clathrate hydrate formation could be inhibited if some means for blocking this process could be found.

In conclusion, we have shown, for the first time by a single investigative technique, the local structural correlations involved in the formation of a clathrate hydrate from a liquid under inert gas applied pressure. The results clearly demonstrate the similarities and differences between the hydrophobic hydration shell of the noble gas atom in the liquid state and that found in the solid clathrate. We believe this to be the first ever direct experimental test of the classic iceberg model of Frank and Evans [8]. The result is consistent with that of a neutron scattering study of the hydration of methanol [14] in which it was shown that the degree of disorder in the first hydration shell of a hydrophobic residue was greater than expected in the standard theory.

Furthermore, this novel x-ray absorption spectroscopy measurement demonstrates that one can directly probe the formation and local structural correlations of gas hydrate systems.

*Present address: European Synchrotron Radiation Facility, B.P. 220, 38043 Grenoble cedex, France.

[1] See the news article by M. Mukerjee [Sci. Am. **275**, No. 6, 33 (1996)].

[2] E. D. Sloan, *Clathrate Hydrates of Natural Gases* (Marcel Dekker, New York, 1990).

[3] D. W. Davidson, in *Water—A Comprehensive Treatise,* edited by F. Franks (Plenum, New York, 1973), Vol. 2, p. 115.

[4] G. A. Jeffrey, *An Introduction to Hydrogen Bonding* (Oxford University Press, New York, 1997).

[5] P. M. Rodger, Mol. Simul. **5**, 315 (1990).

[6] H. Tanaka and K. Kiyohara, J. Chem. Phys. **98**, 4098 (1993).

[7] D. W. Davidson, Y. P. Handa, C. I. Ratcliffe, J. S. Tse, and B. M. Powell, Nature (London) **311**, 142 (1984).

[8] H. S. Frank and M. W. Evans, J. Chem. Phys. **13**, 507 (1945).

[9] W. Blokzijl and J. B. F. N. Engberts, Angew. Chem., Int. Ed. Engl. **32**, 1545 (1993).

[10] A. Filipponi, D. T. Bowron, C. Lobban, and J. L. Finney, Phys. Rev. Lett. **79**, 1293 (1997).

[11] A. Filipponi, A. Di Cicco, and C. R. Natoli, Phys. Rev. B **52**, 15 122 (1995).

[12] P. D'Angelo, A. Di Nola, A. Filipponi, N. V. Pavel, and D. Roccatano, J. Chem. Phys. **100**, 985 (1994).

[13] A. Filipponi, J. Phys. Condens. Matter **6**, 8415 (1994).

[14] A. K. Soper and J. L. Finney, Phys. Rev. Lett. **71**, 4346 (1993).